J|A|C|S COMMUNICATIONS

Published on Web 02/04/2009

Optical Characterizations and Electronic Devices of Nearly Pure (10,5) Single-Walled Carbon Nanotubes

Li Zhang,[†] Xiaomin Tu,[‡] Kevin Welsher,[†] Xinran Wang,[†] Ming Zheng,*[,‡] and Hongjie Dai*[,†]

Department of Chemistry and Laboratory for Advanced Materials, Stanford University, Stanford, California 94305, and DuPont Central Research and Development, Wilmington, Delaware 19880

Received December 10, 2008; E-mail: Ming.Zheng@USA.dupont.com; hdai1@stanford.edu

Single-walled carbon nanotubes (SWNTs) have attracted phenomenal attention because of their potential applications in nanoelectronics,[1] drug delivery,[2] and biosensors.[3] The properties of SWNTs depend strongly on tube chirality and diameter. Large-diameter semiconducting tubes are preferred for nanoelectronics since they form good contact with the electrodes and can carry large currents.[4] Recently, chromatography methods have been reported to separate small SWNTs ($\leq$0.9 nm) according to their diameter, chirality, and length. Unfortunately, the efficiency of this method decreased with increasing tube diameter when the established ssDNA sequence $d(GT)_n$ ($n = 10-45$)[5−10] was used. The performance of the field-effect transistors (FETs) made with these tubes was limited because of their small diameter,[9] demonstrating the need for better chirality separation of large-diameter SWNTs for high-performance nanoelectronics.

Here we report ion-exchange (IEX) separation of (10,5) SWNTs (diameter = 1.03 nm) for application in nanoelectronic devices. A systematic search of DNA sequences for improving IEX separation of DNA−CNT hybrids was performed. This led to the identification of a set of ssDNA sequences, each of which, when used to form hybrids with HiPco tubes, allows particular (*n*,*m*) semiconducting tubes to elute first among all species during an IEX run, resulting in purification of the desired (*n*,*m*) species. All 12 major types of semiconducting tubes present in the starting HiPco material were purified in this way. A detailed account of the work will be given elsewhere.[11] The (10,5) tubes had the largest diameter among the 12 types of purified tubes and thus was chosen for FET device fabrication. It was obtained with the 13-mer ssDNA sequence $(TTTA)_3T$. In addition to the electrostatic properties of the DNA−CNT hybrid, which serves as the foundation for the IEX purification method, we propose that the unique recognition ability of $(TTTA)_3T$ for (10,5) tubes allows them to form a structurally well-defined complex and elute in early fractions.

The IEX procedure is similar to what was previously reported.[8] However, it was found that the resolution and recovery of each (*n*,*m*) species can be improved by tuning the composition and pH of the dispersion and elution buffers. For optimum (10,5) purification, 1 mg of ssDNA was added to 1 mg of HiPco tubes (lot R0217, CNI, Houston, TX) in 1 mL of 0.1 M sodium acetate buffer (pH 4.5) and incubated for 2 days before centrifugation. The supernatant solution collected after centrifugation was then fractionated through an IEX column (Biochrom, Terre Haute, IN) with 2× SSC (0.3 M NaCl, 0.03 M sodium citrate)/0.5 mM EDTA (pH 7.0) and a 0−1 M sodium benzoate gradient.

The AFM image (Figure 1a) illustrates the purity and length distribution of the separated tubes. They all have the same height, suggesting uniform diameter. The UV−vis spectrum in Figure 1b shows the E_{11} transition at 1278 nm, the E_{22} transition at 798 nm, and the E_{33} transition at 386 nm, with E_{11} and E_{22} slightly red-shifted from the semiempirical values (1250 nm, 786 nm) for (10,5) tubes suspended in SDS.[12] The lack of absorption peaks in the 400−600 nm region indicates that the amount of metallic SWNTs present in the sample is small and below the UV−vis detection limit. The resonance Raman spectrum shown in the inset of Figure 1b is the average of spectra collected from hundreds of tubes deposited on a silicon substrate. Only one RBM peak at 233 cm^{-1} is shown, corresponding to the (10,5) tubes. The photoluminescence-versus-excitation (PLE) spectra shown in Figure 1c provide further information about the purity of the tubes. PLE spectra can clearly distinguish similar-diameter semiconducting SWNTs with different chiralities contributing to the same E_{11} absorption peak. The single

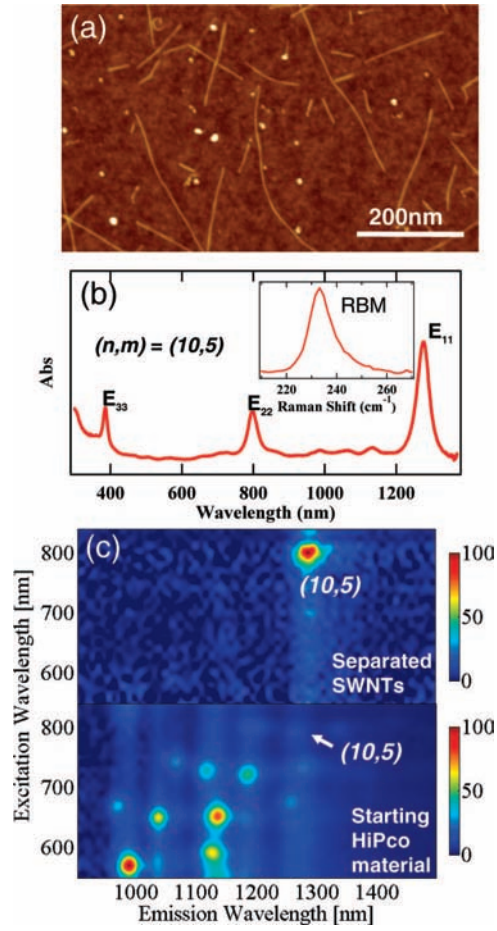

Figure 1. (a) AFM image of the (10,5) SWNTs, (b) optical absorption spectrum of the (10,5) SWNTs (inset: Raman spectrum), and (c) PLE spectra of (top) the (10,5) SWNTs and (bottom) the starting HiPco material.

[†] Stanford University.
[‡] DuPont Central Research and Development.

10.1021/ja8096674 CCC: $40.75

peak in the spectrum further confirms the single-chirality property of the sample. From Figure 1c, one can see that there are few (10,5) tubes in the starting HiPco material. Other starting materials, such as laser ablation tubes, are needed to obtain separated large quantities of (10,5) SWNTs and other larger SWNTs.

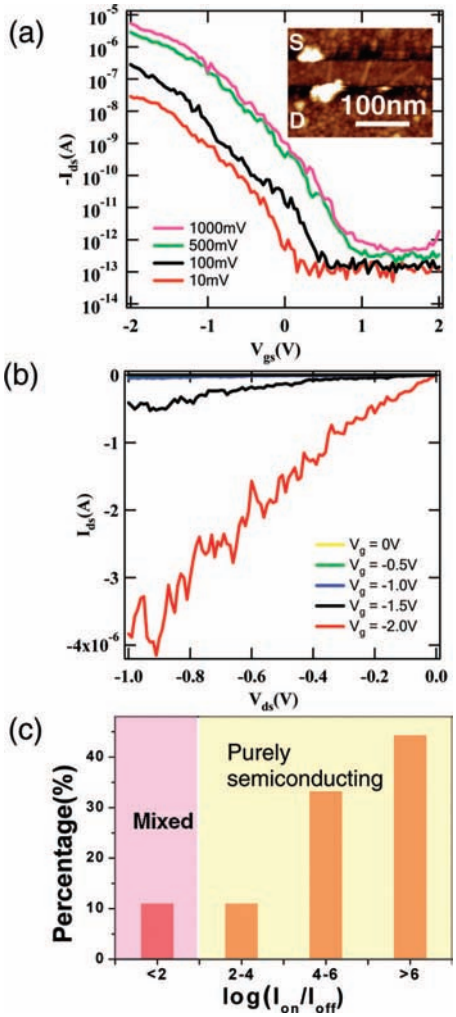

Figure 2. Electrical transport properties of FETs made of chemically separated SWNTs. (a) Transfer characteristics ($I_{ds}-V_{gs}$ curves) of a typical device made of ~15 (10,5) SWNTs at different bias voltages. The inset shows an AFM image of part of the device. (b) Current−voltage characteristics ($I_{ds}-V_{ds}$) of the device at different values of V_{gs}. (c) Histogram of the percentages of devices with various I_{on}/I_{off} ratios (total number of devices = 60).

The electrical properties of the FETs made with the chromatographically separated (10,5) SWNTs are shown in Figure 2. The channel length of the devices is ~80−100 nm. AFM imaging of the devices shows that each device is connected by ~15 tubes on average (Figure 2a inset). The I_{on}/I_{off} ratio of a typical device is as high as 10^6 (Figure 2a). Figure 2b shows that the on current at a bias of 1.0 V is ~4 μA, which is significantly higher than our previously reported result (~1 μA) for the device with a longer channel (~200−300 nm) and smaller tubes (~0.8−0.9 nm).[9] The performance improvement is mainly due to the larger diameter of the SWNTs, which results in a smaller band gap and smaller contact barriers with the electrodes. The I_{on}/I_{off} statistics of more than 60 devices shows that half of the devices have an I_{on}/I_{off} ratio of greater than 10^6 (Figure 2c). Around 88% of the devices exhibit $I_{on}/I_{off} > 10^2$, indicating that all of the SWNTs (average number ~15) in each of these devices are semiconductors (Figure 2c). This suggests that ~99% (i.e., $0.99^{15} \approx 88\%$) of the SWNTs in the separated SWNTs are semiconductors, of which almost all are (10,5) tubes according to the PLE spectra (Figure 1c). In other words, semiconducting (10,5) SWNTs are highly enriched, leading to depletable FET devices composed of SWNTs with the same chirality. The 99% enrichment of (10,5) tubes is highly improved over the previous result of 94% enrichment of (7,6) and (8,4) tubes using the $d(GT)_{20}$ DNA.[9] This is the first time that SWNT FETs with single chirality and diameter ≥1 nm have been achieved.

In summary, SWNTs with specific chirality (10,5) were recognized by the ssDNA sequence $(TTTA)_3T$ and eluted first during IEX. The separation efficiency was highly improved compared with previously reported results using $d(GT)_{20}$. The separation result was characterized with UV−vis, Raman, and PLE spectroscopy, all of which revealed nearly pure (10,5) SWNTs. Nanoelectronic devices were fabricated with I_{on}/I_{off} ratios as high as 10^6 due to the single-chirality-enriched (10,5) tubes. While the performance of the FETs made with the slightly bigger (10,5) tubes is better than the previously reported results using (7,6) and (8,4) tubes, even larger single-chirality semiconducting SWNTs are preferred in order to further improve the device performance. We have identified a sequence motif that has the potential to purify single-chirality SWNTs. Applying these sequences to laser-ablation SWNTs may purify other large-diameter tubes.

Acknowledgment. This work was supported by MARCO-MSD, Intel, and NSF Grant CMS-060950.

Supporting Information Available: Details regarding the absorption and photoluminescence excitation measurements, Raman spectroscopy, AFM, and electrical device fabrication and characterization. This material is available free of charge via the Internet at http://pubs.acs.org.

References

(1) Javey, A.; Guo, J.; Wang, Q.; Lundstrom, M.; Dai, H. *Nature* **2003**, *424*, 654–657.
(2) Kam, N. W. S.; Dai, H. *J. Am. Chem. Soc.* **2005**, *127*, 6021–6026.
(3) Chen, R. J.; Bangsaruntip, S.; Drouvalakis, K. A.; Kam, N. W. S.; Shim, M.; Li, Y. M.; Kim, W.; Utz, P. J.; Dai, H. J. *Proc. Natl. Acad. Sci. U.S.A.* **2003**, *100*, 4984–4989.
(4) Kim, W.; Javey, A.; Tu, R.; Cao, J.; Wang, Q.; Dai, H. *Appl. Phys. Lett.* **2005**, *87*, 173101.
(5) Tu, X.; Zheng, M. *Nano Res.* **2008**, *1*, 185–194.
(6) Zheng, M.; Jagota, A.; Semke, E. D.; Diner, B. A.; Mclean, R. S.; Lustig, S. R.; Richardson, R. E.; Tassi, N. G. *Nat. Mater.* **2003**, *2*, 338–342.
(7) Zheng, M.; Jagota, A.; Strano, M. S.; Santos, A. P.; Barone, P.; Chou, S. G.; Diner, B. A.; Dresselhaus, M. S.; Mclean, R. S.; Onoa, G. B.; Samsonidze, G. G.; Semke, E. D.; Usrey, M.; Walls, D. J. *Science* **2003**, *302*, 1545–1548.
(8) Zheng, M.; Semke, E. D. *J. Am. Chem. Soc.* **2007**, *129*, 6084–6085.
(9) Zhang, L.; Zaric, S.; Tu, X.; Wang, X.; Zhao, W.; Dai, H. *J. Am. Chem. Soc.* **2008**, *130*, 2686–2691.
(10) Li, X.; Zhang, L.; Wang, X.; Shimoyama, I.; Sun, X.; Seo, W. S.; Dai, H. *J. Am. Chem. Soc.* **2007**, *129*, 4890–4891.
(11) Tu, X.; et al. Manuscript in preparation.
(12) Bachilo, S. M.; Strano, M. S.; Kittrell, C.; Hauge, R. H.; Smalley, R. E.; Weisman, R. B. *Science* **2002**, *298*, 2361–2366.

JA8096674